Investigation of the RCS for Finite Bandpass Frequency Selective Surface

Chengran Fang [2], Xiuzhu Ye [1], Yan Zhang [4], Qian Wang [3], Jingcheng Zhao [4], Naixin Zhang [4], Hao Jiang [4], Cheng Jin [1], and Ming Bai [4]

[1] Department of Electronics and Information Engineering
Beijing Institute of Technology, Beijing, 100081, China
xiuzhuye@outlook.com

[2] Sino-French Engineer School
Beihang University, Beijing, 100191, China

[3] The Aeronautical Science Key Lab of High-Performance Electromagnetic Windows
The Research Institute for Special Structures of Aeronautical Composite AVIC, Jinan, 250023, China

[4] Department of Electronics and Information Engineering
Beihang University, Beijing, 100191, China

Abstract ─ Frequency selective surface (FSS) with finite size behaves differently compared to an ideal infinite one, due to the influence of fringe effect, while there exist little study concerning this subject. RCS radiation can serve as a critical indicator of the FSS performance which can quantitatively reveal the mechanism of the fringe effect. This paper presents the study of RCS for FSS with finite structures. RCS for different sized FSS with different configurations under plane wave illumination are studied qualitatively. The result reveals the frequency selectivity and fringe effect of finite FSS. Quantitative functional relations between fringe effect and dimension of FSS are first summarized for monolayer FSS. A new case is then picked and tested to verify the validity of the functional relations. The relations are also extended to multilayer FSS. It turns out that the relations are general properties of finite FSS excited by plane waves.

Index Terms ─ Finite FSS, fringe effect, multilayer FSS, RCS.

I. INTRODUCTION

Frequency selective surface (FSS) is a kind of spatial filtering structure, through which the electromagnetic wave of a specific frequency range can pass, while the others are reflected. Basically, an ideal frequency selective surface is composed of identical patches or unit elements periodically arranged in a two-dimensional infinite array. The special electromagnetic properties possessed by FSS is unique in the electromagnetic domain. FSSs are able to react differently to electromagnetic waves according to frequency, angle of incidence and polarization. Therefore, FSS can behave as "spatial" filters. By well designing the structure of FSS, we can adjust their behaviors in order to satisfy some engineering requirements.

A large variety of FSS is used in parabolic antennas, radomes, THz technologies, etc. In general, there are two main usages of FSS, one of them is to realize the frequency multiplexing, the other is to reduce the RCS of a structure, or stealth technology [1,2]. According to the number of layers, FSS can be divided into monolayer FSS and multilayer FSS. Monolayer FSS contains only one layer of the periodic structure and is easy to be machined. Therefore, it is well developed and widely used. Figure 1 presents some examples of different types of unit elements [1]. It should be noticed that the complementary of these elements are also eligible FSS units due to Babinet's principle.

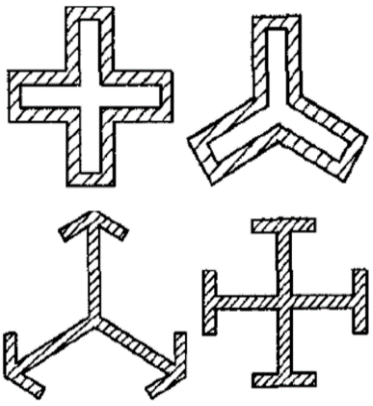

Fig. 1. Four examples of FSS unit elements.

Submitted On: October 14, 2018
Accepted On: April 1, 2019

However, monolayer FSS is hard to achieve large constant bandwidth, flat top and fast roll-off. A multilayer FSS is the combination of a series of well-designed monolayer FSS. One of the motivations for multilayer FSS is to incorporate different properties of each FSS layers. Thus, multilayer FSS can achieve large bandwidth and fast roll-off more easily than a single monolayer FSS [3]. The design and performance analysis of multilayer FSS become the main trend of contemporary research [4]. Therefore, to evaluate the fringe effect for both types of FSSs, in this paper, we have chosen a bandpass FSS with cross aperture units for monolayer FSS, and a broad bandwidth bandpass filter designed in [5] for multilayer FSS. The dimension and configuration of these FSS are presented in Section II.

Traditional research methods usually assume that the FSS is an infinite array. Because of fringe effect, the actual electrical performance of the finite FSS differ from theoretical predictions, and one cannot take full advantage of FSS peculiarities. In order to manipulate the finite FSS, additional attention should be paid to the perturbation caused by the fringe effect. Radar cross-section (RCS) is a measure of detectability of an object [6,7]. Since FSS is an important component of stealth technology, bi-static RCS is chosen as a key indicator of eligibility of FSS [8] to reveal the scattering mechanism of the fringes quantitatively. Hence, a profound comprehension of the bi-static RCS formed by excited FSS is necessary, and we will concentrate on the RCS deform caused by the fringe effect.

In this paper, we study the RCS of finite FSS by simulating a series of finite FSS in commercial software CST. Qualitative analyses about the propagation of E field and bi-static RCS are first conducted to show the fringe effect of finite FSS. The main lobe magnitude and angular width of RCS are then analyzed quantitatively. The main contribution of this paper is that the relations between the dimension of FSS and the fringe effect is summarized and validated. This work can serve as theoretical guidance to the designing and machining of FSS which is finite in size practically.

II. FSS CONFIGURATION

In this study, a unit element with cross aperture is chosen for monolayer FSS. Figure 2 illustrates the dimensions of one unit. We first investigate the frequency selectivity of this unit element. Regarding S-parameters of infinite FSS composed of this unit, the periodic boundary condition is applied to the unit in the simulation. As shown in Fig. 4, the unit element forms into a monolayer FSS with passband 8-12 GHz.

For multilayer FSS, we have chosen an FSS unit composed of 5 layer patches and two types of dielectric mediums as illustrated in Fig. 3. The round or hollow patches are 5 FSS units, and the red and blue materials are dielectric mediums (Some parts of the multilayer FSS are set to be solid red in Fig. 3 to emphasize the 3D structure of FSS). The geometric parameters of the multilayer FSS are as listed in Table 1.

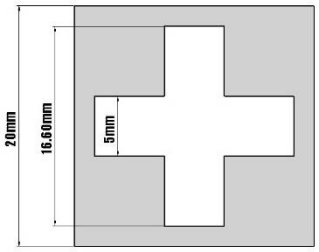

Fig. 2. The dimension of square FSS with cross aperture.

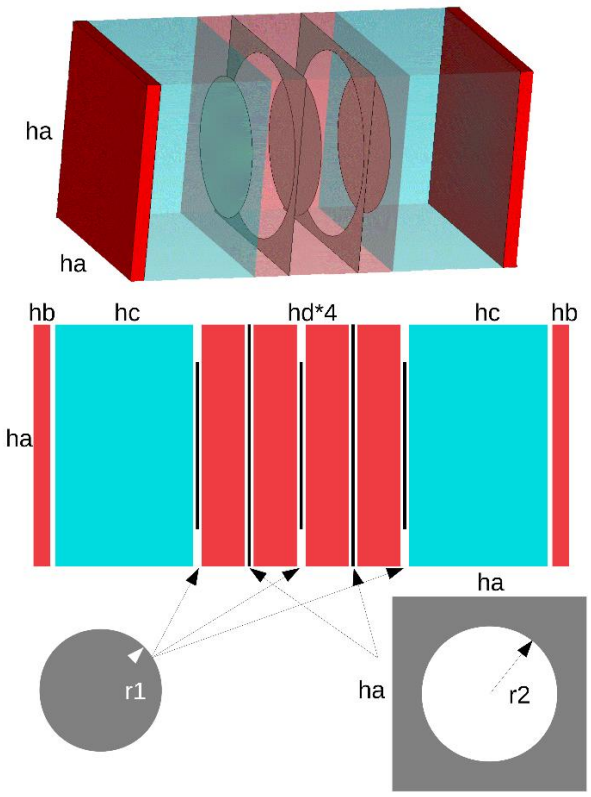

Fig. 3. The configuration of the multilayer FSS unit.

Table 1: Geometric parameters of multilayer FSS (mm)

ha	hb	hc	hd	r1	r2
8.4	0.6	4.8	1.5	2.9	3.8

Similarly, the periodic boundary condition is applied in order to obtain S-parameters of the multilayer FSS (see Fig. 4). It is evident that the bandwidth of the multilayer FSS is large and flat with passband 8-12 GHz. In this study, different sized FSS are excited by plane wave at frequency ranging from 5 GHz to 15 GHz, and three frequency points (5, 10, 15 GHz) in the passband and stopband are selected deliberately.

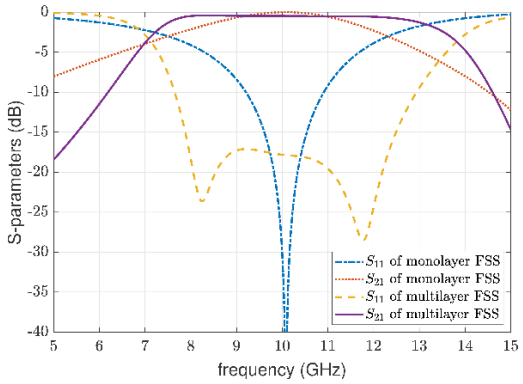

Fig. 4. S-parameters of infinite FSS.

III. QUALITATIVE ANALYSIS OF RCS

Before we conduct RCS analysis of FSS, it is helpful to verify the frequency selectivity of FSS and get the first impression of fringe effect. Two finite monolayer FSS with different number of units are excited by plane wave with frequency ranging from 5 GHz to 15 GHz. Figure 5 illustrates the propagation of E field sampling in the three frequency points (5, 10, 15 GHz). Left images are results of small size (5x5 units) FSS and right images are results of large size (10x10 units) FSS.

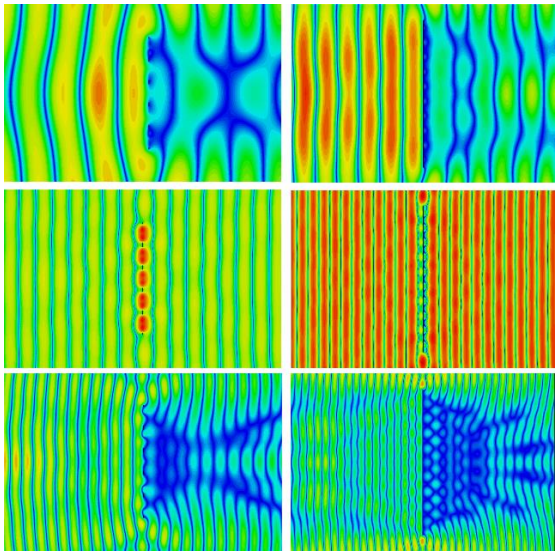

Fig. 5. E field propagation with 5x5 units FSS (left), 10x10 units FSS (right) in 5 GHz (first row), 10 GHz (second row) and 15 GHz (third row).

It is clear that all sizes of FSS present a frequency selectivity and fringe effect. In fact, the incident plane wave will be partly reflected by FSS in the backward direction and partly transmitted in the forward direction. At passband, the incident wave should pass through the FSS totally without reflection. At stopband, the incident wave should be reflected back and there should be no wave at the back of the FSS. Due to the diffraction of electromagnetic wave around finite FSS, the cancellation cannot be perfect, and the deform of plane wave can be observed in Fig. 5.

Concerning the bi-static RCS analysis, we first compare RCS simulation results of finite FSS, perfect electric conductor (PEC) slab and dielectric slab in order to analyze the transmission performance of FSS. The relative permittivity of the dielectric slab is 1.2. Moreover, the sizes of the PEC slab and dielectric slab are the same as the comparative finite FSS. Figures 6 and 7 show the bi-static RCS simulation results for 5x5 monolayer and 12x12 multilayer FSS.

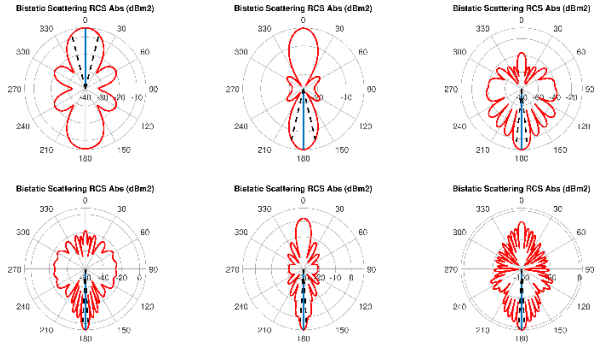

Fig. 6. Bi-static RCS of monolayer FSS (left), PEC (center) and dielectric slab (right) in 5 GHz (first row) and 10 GHz (second row).

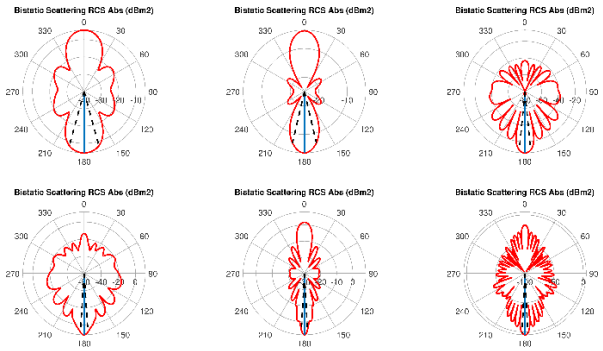

Fig. 7. Bi-static RCS of multilayer FSS (left), PEC (center) and dielectric slab (right) in 5 GHz (first row) and 10 GHz (second row).

It can be seen that the bi-static RCS of both monolayer and multilayer FSS are similar to that of PEC in the stopband and resemble that of the dielectric slab in the passband. This phenomenon can be explained by the physical bandpass property of the FSS. The differences between them mainly lie in the magnitude and the angular width of the main lobe and shape of the side lobe. A further study also shows that the bigger the size of FSS is, the smaller the differences are in both stopband and

passband. As a result, we can concentrate on the main lobe study in the quantitative analysis.

IV. QUANTITATIVE ANALYSIS OF RCS

A. Main lobe magnitude

In this section, we will study the relationship between the main lobe magnitude of RCS and the dimension of FSS. Main lobe magnitude is the maximal value in the main lobe of RCS which represents the intensity of the transmitted or reflected wave. As we found in Section III, the fringe effect will badly reduce the magnitude of main lobe in both passband and stopband. Therefore, it is worthy to find a quantitative relation of main lobe magnitude and the dimension of FSS.

In order to capture the physical and electrical size of FSS, we introduce a dimensionless quantity,

$$\alpha = \frac{FSS\ surface}{FSS\ perimeter \times wavelength}, \quad (1)$$

to quantify the FSS dimension. Within the formula, FSS surface quantifies the area of the finite FSS including areas of apertures and conductors; FSS perimeter is the whole length of the border around finite FSS. RCS of each FSS is simulated and sampled at different frequencies.

We first study the main lobe magnitude of RCS generated by a group of different sized monolayer FSS. The quantitative relations of the main lobe magnitude with respect to α are shown in Fig. 8. Three frequency points (5, 10, 15 GHz) are chosen. It can be verified that the larger α is, the larger is the magnitude of main lobe and the less is the fringe effect.

Besides, we fit the results to third degree polynomials in order to quantitatively capture the fringe effect. It turns out that the relations between α and main lobe magnitude can be properly represented by third degree polynomials since the correlation coefficients are all very close to 1. The case of 30x30 FSS, which is out of the range of the training set, is also simulated and predicted to verify the prediction performance of the curves. Table 2 shows the result. The relatively small errors present the good performance of prediction formula.

Furthermore, the third-degree polynomial relation can be extended to multilayer FSS. The RCS main lobe of different sized multilayer FSS which are excited by plane wave are simulated. The same pattern is also found in this case. Figure 9 provides the figures of RCS main lobe magnitude in relation to multilayer FSS dimension. The polynomial pattern is clear, and this fact generates the result found in monolayer FSS to multilayer FSS.

B. Angular width

In addition to the main lobe magnitude, the angular width of RCS main lobe which represents the directivity of the reflected or transmitted wave is also a key factor of FSS. The angular width is defined as the angle between the two directions where the radiation is dropped by 3 dB regarding the maximum radiation in the main lobe direction [6].

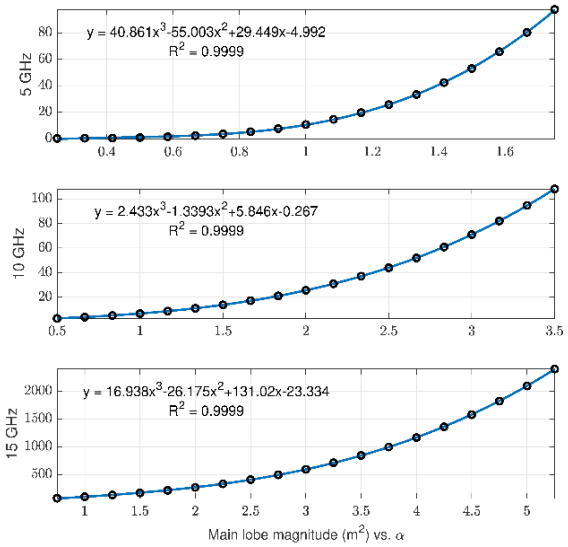

Fig. 8. The relations between the main lobe magnitude and the dimension of monolayer FSS.

Table 2: Comparison between true values of main lobe magnitude and predicted values

30x30 FSS	True Values	Predicted Values	Error
5 GHz	$395m^2$	$363.3m^2$	8.02%
10 GHz	$314m^2$	$299.6m^2$	4.58%
15 GHz	$6920m^2$	$6632.7m^2$	4.15%

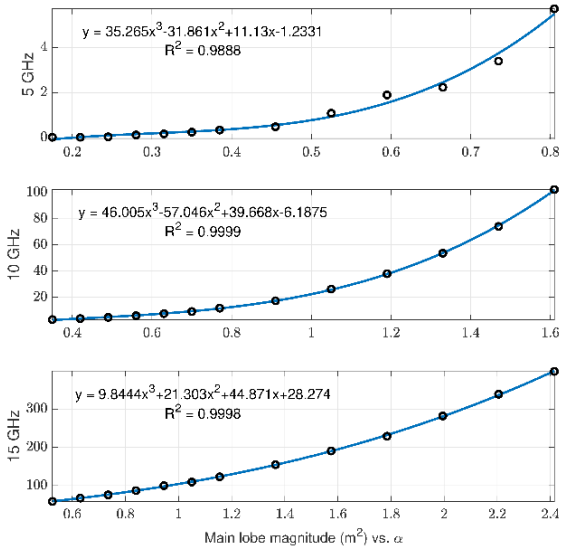

Fig. 9. The relations between the main lobe magnitude and the dimension of multilayer FSS.

Different sized monolayer FSS are excited by plane wave, and we calculate the angular width of RCS main lobe. The relations between angular width and dimension of FSS in 3 frequencies are illustrated in Fig. 10. It can be seen that the angular width shrinks with the increase of FSS dimension. This means that the directivity of transmitted wave ameliorates with the enlargement of FSS size. The fact fits our intuition since the transmitted wave is a plane wave with impulse function shaped RCS for an infinite FSS.

We also fit the results to three polynomial equations. The polynomial equations and correlation coefficients are presented in Fig. 10. We found that the angular width is inversely proportional to the dimension of monolayer FSS and the correlation coefficients are quite close to 1. In order to verify the prediction performance, we compare the true value with the predicted value in the case of 30x30 FSS in Table 3.

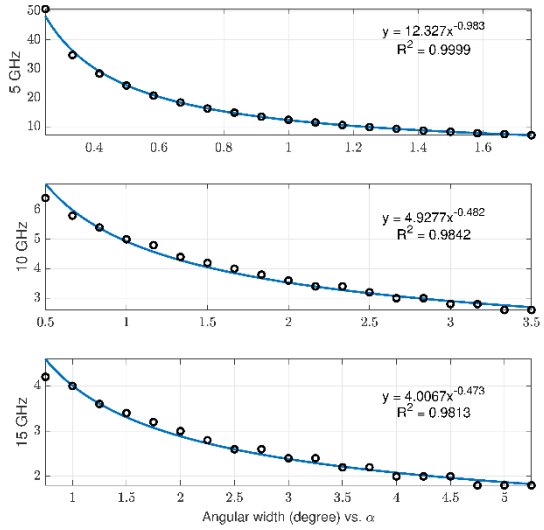

Fig. 10. The relations between the main lobe magnitude and the dimension of multilayer FSS.

Table 3: Comparison of true value of main lobe magnitude and predicted value

30x30 FSS	True Value	Predicted Value	Error
5 GHz	5	5.01	0.16%
10 GHz	2	2.27	13.4%
15 GHz	1.4	1.54	10.3%

Moreover, the inversely proportional relation can also be generated to multilayer FSS. In the case of multilayer FSS illuminated by plane wave, we plot the angular width with respect to FSS dimension (see Fig. 11). We can also find the inversely proportional relation with high correlation coefficient.

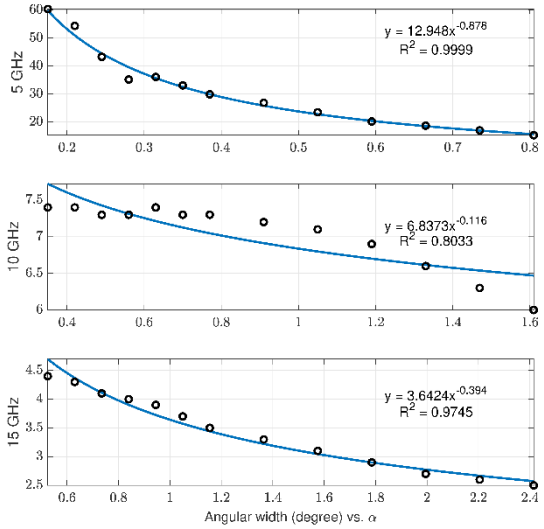

Fig. 11. The relations between the main lobe magnitude and the dimension of multilayer FSS.

V. CONCLUSION

This paper presents a study of RCS properties for finite FSS. Some main characters of RCS for frequency selective surfaces are captured in the analyses. We choose two typical bandpass FSS representing monolayer FSS and multilayer FSS respectively. A qualitative analysis is first conducted. The simulations reveal that the selectivity of FSS and fringe effect will perturb RCS radiation of finite FSS. Some quantitative relations are found afterward, and the relations are verified by concrete instances. The fitted curve found in monolayer FSS can also be extended to multilayer FSS. It means that the discovered relations are general properties of finite FSS regardless of the FSS design. The result can serve as a guideline for design and machining of practical FSS.

ACKNOWLEDGMENT

This work is supported by the National Natural Science Foundation of China under Grant No. 61401009 and Grant No. 61671032 and the Aeronautical Science Foundation of China under Grant 20161851009.

REFERENCES

[1] B. A. Munk, *Frequency Selective Surfaces: Theory and Design*. John Wiley & Sons, 2005.

[2] A. N. Silva, et al., "Simple and efficient design of reconfigurable FSS with triangular patch elements," *Applied Computational Electromagnetics Society Symposium-Italy (ACES), 2017 International, IEEE*, 2017.

[3] B. Liang and M. Bai. "Subwavelength three-dimensional frequency selective surface based on

surface wave tunneling," *Optics Express*, vol. 24, no. 13 pp. 14697-14702, 2016.

[4] M. Jin and M. Bai. "On the transmitted beam degradation through FSS in the working band by plane-wave spectrum computation and evaluation," *Applied Computational Electromagnetics Society Journal*, vol. 31, no. 9, 2016.

[5] X. Liu, et al., "On the improvement of angular stability of the 2nd-order miniaturized FSS structure," *IEEE Antennas and Wireless Propagation Letters*, vol. 15, pp. 826-829, 2016.

[6] E. F. Knott, *Radar Cross Section Measurements*. Springer Science & Business Media, 2012.

[7] J. Su, et al., "Ultra-wideband and polarization-insensitive RCS reduction of microstrip antenna using polarization conversion metasurface," *Applied Computational Electromagnetics Society Journal*, vol. 32, no. 6, 2017.

[8] R. Mittra, C. H. Chan, and T. Cwik, "Techniques for analyzing frequency selective surfaces-A review," *Proceedings of the IEEE*, vol. 76, no. 12, pp. 1593-1615, 1998.

Chengran Fang received the B.S. degree from Sino-French Engineer School, Beihang University, Beijing, China, in 2016. He is currently working towards the M.S. degree with the Department of Electronics and Information Engineering, Beihang University, Beijing.

His research interests include computational electromagnetics, inverse problem and machine learning.

Xiuzhu Ye (S'11-M'12) received the B.E. degree in Telecommunication Engineering from Harbin Institute of Technology, Harbin, China, in 2008 and the Ph.D. degree from Department of Electrical and Computer Engineering in National University of Singapore, Singapore, in 2012.

From 2012 to 2013, she worked in Department of Electrical and Computer Engineering, National University of Singapore as a Research Fellow. Since 2013, she worked as Assistant Professor in Beihang University. Since 2019, she has been an Associate Professor with School of Information and Electronics, Beijing Institute of Technology. Her research areas are electromagnetic inverse problems, microwave imaging methods, antenna designing and radar techniques.

Ye has served on review boards of various technical journals, including IEEE Transactions on Antenna and Propagation, IEEE Transactions on Microwave Theory and Techniques, Radio Science and Optics Express.